Nanoscale

Poly(lactic acid) stereocomplex microspheres as thermally tolerant optical resonators

Journal:	*Nanoscale*
Manuscript ID	NR-COM-10-2023-005318
Article Type:	Communication
Date Submitted by the Author:	21-Oct-2023
Complete List of Authors:	Suharman, Suharman; University of Tsukuba, Graduate School of Pure and Applied Sciences Heah, Wey; University of Tsukuba Faculty of Pure and Applied Sciences, Division of Materials Science Yamagishi, Hiroshi; University of Tsukuba Faculty of Pure and Applied Sciences, Division of Materials Science Yamamoto, Yohei; University of Tsukuba, Graduate School of Pure and Applied Sciences

COMMUNICATION

Poly(lactic acid) stereocomplex microspheres as thermally tolerant optical resonators

Received 00th January 20xx,
Accepted 00th January 20xx

DOI: 10.1039/x0xx00000x

Suharman[a,b], Wei Yih Heah[c], Hiroshi Yamagishi[a,c], and Yohei Yamamoto*[a,c]

Thermally tolerant polymer optical resonators are fabricated from stereocomplex of poly(L-lactic acid) and poly(D-lactic acid) through oil-in-water miniemulsion method. The thermal stability of the microspheres of the stereocomplex poly(lactic acid) (SC-PLA) is superior to those of the homochiral poly(lactic acid) (HC-PLA). As a result of the high thermal stability, optical resonator properties of the SC-PLA microspheres preserve at elevated temperature up to 230 °C, which is higher by 70 °C than that of microspheres formed from HC-PLA.

Poly(lactic acid) (PLA) is a synthetic polyester made from lactic acid.[1–4] Due to the biodegradable, biocompatible, and nontoxic properties, PLA is widely used for biomedical applications,[5–7] drug transportation,[8] textile, [9] and packaging.[10,11] PLA has three types of stereoisomers; poly(L-lactide acid) (PLLA), poly(D-Lactide acid) (PDLA), and their atactic polymer, poly(DL-lactic acid)(PDLLA).[12] The homopolymers of PLLA and PDLA form semicrystalline aggregates with a melting temperature at around 170 °C, while the atactic PDLLA copolymer forms an amorphous aggregate with a lower melting temperature.[13]

One of the drawbacks of PLA is that the thermal stability of PLA is not so high due to its low crystallinity, which limits the use of PLA in optical and electronic applications[14]. Some techniques have been applied to enhance the thermal stability of PLA by adding a nucleating agent,[15–18] physical modification through fibre reinforcement,[19,20] the addition of inorganic particles[21], chemical modification,[22] and blending with the material with high T_g and high heat resistance,[23,24] In particular, stereocomplexation by mixing PLLA and PDLA have been received much attention due to its enhanced thermal and mechanical properties.[25, 26] A mixture of PLLA and PDLA, prepared from its molten state or solution state, induces the formation of stereocomplex PLA (SC-PLA) driven by the intensive intermolecular hydrogen (H)-bonding and dipole-dipole interactions between PLLA and PDLA (**Fig. 1**).[27–29] Compared with homochiral PLA (HC-PLA), SC-PLA has a melting temperature (T_m) of around 230 °C, which is higher than that of the pure HC-PLA (~170 °C), since the intermolecular H-bonding interaction between PLLA and PDLA chains increases the rigidity of the PLA chains.[30–35]

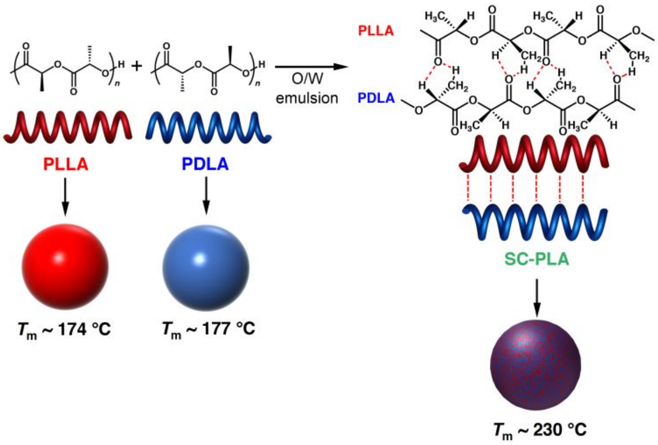

Fig. 1. Schematic illustration of fabrication of microspheres from HC- and SC-PLA by O/W emulsion method.

Optical resonators confine light in a small volume that interferes to show up sharp optical signals.[36] Typical optical resonators are Fabry-Pérot (F-P) resonators and whispering gallery mode (WGM) resonators.[37] For F-P resonators, light is confined between counter mirrors or crystalline facets.[38] On the other hand, WGM resonators confine light circularly by total internal reflection (TIR) at the interface between the inner and outer media with different refractive indices. Typical WGM resonators have shapes of sphere, ring, polyhedron etc.[39] WGM is highly sensitive to the surface morphology, because a rough surface tends to scatter light, which reduce the light confinement efficiency in the resonator.[40] Therefore, highly smooth surface is one of important factors for the high quality factor (Q) microresonators. The sharp PL peaks from the

a. Department of Material Innovation, Graduate School of Pure and Applied Science, University of Tsukuba, 1-1-1 Tennodai, Tsukuba, Ibaraki, 305-8573, Japan.
b. Department of Chemistry, Faculty of Mathematics and Natural Science, Universitas Sumatera Utara. Jl. Dr. T. Mansur No. 9, Padang Bulan, Medan Baru, Medan, Sumatera Utara 20222, Indonesia.
c. Department of Material Science, Institute of Pure and Applied Science, University of Tsukuba, 1-1-1 Tennodai, Tsukuba, Ibaraki, 305-8573, Japan.
E-mail: yamamoto@ims.tsukuba.ac.jp
Electronic Supplementary Information (ESI) available: [details of any supplementary information available should be included here]. See DOI: 10.1039/x0xx00000x

resonators are utilized for highly sensitive chemical and biosensing applications by monitoring the peak shift.[41,42]

In this work, we investigate optical resonator properties of the microspheres formed from PLAs. The whispering gallery mode (WGM) microresonators are fabricated from a blend of PLLA and PDLA through oil-in-water (O/W) miniemulsion method. We expect that the microresonators formed from SC-PLA has better thermal stability than the microresonators formed from pure HC-PLA. We find that the WGM resonators from SC-PLA are much more stable even at 230 °C in comparison with those from HC-PLA (~170 °C).

Microspheres of HC-PLA composed of PLLA (the number averaged molecular weight, M_n = 40 kg mol^{-1}) or PDLA (M_n = 90 kg mol^{-1}) were prepared by O/W miniemulsion method. Similarly, microspheres of SC-PLA composed of a blend of PLLA and PDLA were fabricated with the mixing ratio of PLLA to PDLA (L/D) of 9/1, 7/3, 5/5, 3/7, and 1/9. The miniemulsion method is chosen because of the efficient formation of SC-PLA with high reaction rate compared to other methods such as solution blending, supercritical fluid, and melted blending.[32,43] During the emulsification and subsequent solvent evaporation processes, PLLA and PDLA form stereocomplex.

Fig. 2 shows scanning electron microscopy (SEM) images of the resultant microspheres formed from HC- and SC-PLA. All the microspheres have high sphericity but have different surface morphology. The microspheres of HC-PLA with L/D of 10/0 containing only PLLA (**Fig. 2a and b**) and SC-PLA with L/D of 9/1 and 7/3 (**Fig. 2c and d**, respectively) have rather smooth surface with the values of the root-mean-square (RMS) roughness between 4–5 (in details of the calculation of the RMS roughness, see the Supporting Information). The surface of the microsphere becomes rough with the increase of the content of PDLA with L/D of 5/5, 3/7 and 1/9 with the value of the RMS roughness of 6.23, 11.5, and 14.6, respectively (**Fig. 2e-g**). As for the microparticles made from only PDLA (L/D = 0/10), the surface morphology is quite rough with the RMS roughness value as large as 46.3 (**Fig. 2h**). The difference of the surface morphologies of the microspheres from PLLA and PDLA is possibly due to the difference in the molecular weights of these polymers, which causes the different crystallinity of the microspheres.[44]

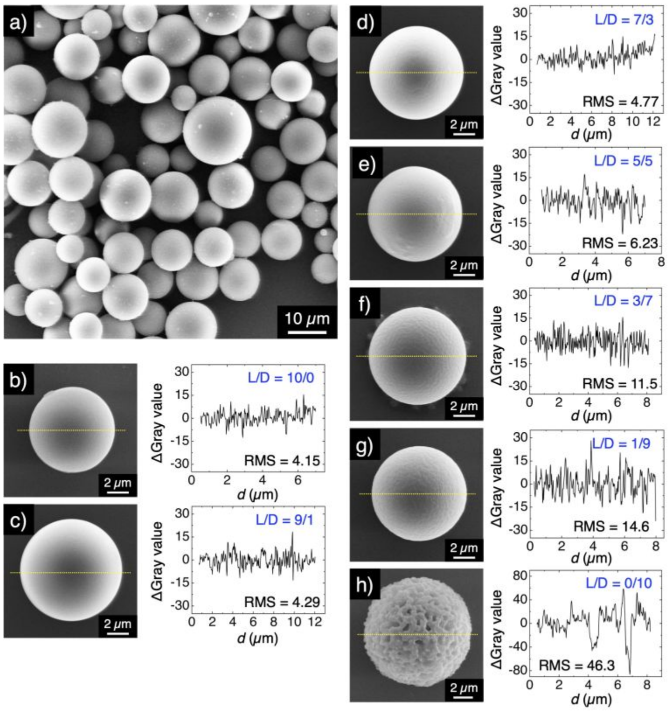

Fig. 2. SEM micrographs of HC-PLA and SC-PLA microspheres prepared by O/W miniemulsion method with different L/D ratios of 10/0 (a, b) 9/1 (c), 7/3 (d), 5/5 (e), 3/7 (f), 1/9 (g), and 0/10 (h). The graphs on the right in (b–h) show profiles of the difference of the gray values versus distance (*d*) at the cross section of the microspheres shown as yellow-dotted lines in the corresponding micrographs.

We investigate the change in the morphology of the microsphere by heating. As shown in **Fig. S1**, the microspheres of HC-PLA (L/D = 10/0 and 0/10) melt when heated at 200 °C for 2 s. However, microspheres of SC-PLA with the L/D ratio of 9/1, 7/3, 5/5, 3/7, and 1/9 keep their spherical morphologies after being heated at 200 °C, indicating that the thermal stability of the PLA is remarkably improved by the SC formation. Even for a microsphere with L/D of 9/1, where the composition of the HC crystallites is greater than that of the SC crystallites, the microsphere preserves its spherical morphology upon heating at 200 °C.

The thermal stability of HC- and SC-PLA microspheres was investigated in more detail by differential scanning calorimetry (DSC). **Fig. 3** shows the DSC thermograms (first heating) of the HC and SC crystallites with the different mixing ratios (L/D = 10/0, 9/1, 7/3, 5/5, 3/7, 1/9, 0/10). Several characteristic endo-/exothermic peaks were observed: Endothermic peaks at 60–70 °C due to the glass transition (T_g), exothermic peaks at 90–110 °C due to the crystallization (T_c), and endothermic peaks at > 170 °C due to the melting of the HC and SC crystallites. For HC-PLA (L/D = 10/0 and 0/10), T_m appears at 174 and 177 °C, respectively. In contrast, for SC-PLA, another peak appeared at 227–230 °C, which is attributed to T_m of the SC crystallites.[25] These results indicate that blending PLLA and PDLA forms both SC and HC domains.

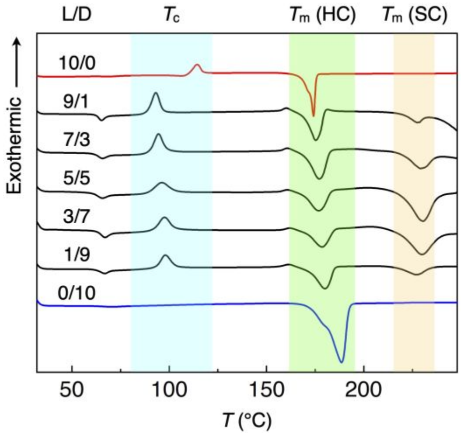

Fig. 3. DSC traces of HC- and SC-PLA with different L/D ratio.

Thermal properties of HC- and SC-PLA are summarized in **Table 1**. From the peak area of T_m in the DSC thermograms, melting enthalpies (ΔH_m) of the HC and SC crystallites are determined. By changing the L/D ratio from 10/0 to 5/5, ΔH_m of HC-PLA (ΔH_{HC}) decreases from 54 to 24 J g^{-1} and then increases to 71 J g^{-1} by further change of the L/D ratio to 0/10. Concomitantly, ΔH_m of SC-PLA (ΔH_{SC}) significantly increases from 9 to 45 J g^{-1} and then decreases to 15 J g^{-1} upon increasing the PDLA content. The ΔH_{HC} and ΔH_{SC} values show minimum and maximum at L/D of 5/5, indicating that PLA mostly forms SC domains in the 5/5 mixture of PLLA and PDLA.[45] Moreover, the decomposition temperatures (T_{dec}) of both HC- and SC-PLA were determined using thermogravimetry differential thermal analysis (TG/DTA, **Fig. S2**). For pure HC-PLLA, T_{dec} was at around 280 °C. As the ratio of PDLA to PLLA increased, T_{dec} increased and reached 337 °C for L/D of 1/9. For pure HC-PDLA, T_{dec} reached to 354 °C. Therefore, T_{dec} is mainly affected by M_n of PLA, where large M_n has high T_{dec}. However, the TGA profiles of SC-PLA show single decomposition step, indicating that the stereocomplex state is not just a simple mixture of PLLA and PDLA but has a strong interaction between PLLA and PDLA via H-bonding (**Fig. 1**).

Table 1. Summary of the thermal behaviour of HC- and SC-PLA microspheres with different L/D ratio

Sample	T_g (°C)	T_c (°C)	T_m, HC (°C)	T_m, SC (°C)	ΔH_{HC} (J g^{-1})	ΔH_{SC} (J g^{-1})
HC-PLA 10/0	-	109	174	-	54	-
SC-PLA 9/1	65	93	176	227	47	9
SC-PLA 7/3	66	95	175	229	24	42
SC-PLA 5/5	66	96	177	230	24	45
SC-PLA 3/7	67	98	177	229	24	41
SC-PLA 1/9	67	98	179	227	33	15
HC-PLA 0/10	-	-	177	-	71	-

To understand the crystalline states of HC- and SC-PLA, powder X-ray diffraction (PXRD) measurements were conducted. As shown in **Fig. 4a**, powder samples of HC-PLA with L/D of 10/0 and 0/10 show diffraction peaks at 2θ = 14.9, 16.7, 19.1, and 22.4°, which are assigned as (010), (110)/(200), (203), (015) of the HC crystallite, respectively. In comparison, powder samples with the blend of PDLA and PLLA exhibit three diffraction peaks additionally at 12.0, 20.8, and 24.1°, which are assigned as (110), (300)/(030), (220) of the SC crystallite, respectively.[25,26,46] For the sample with L/D of 5/5, diffractions from the HC crystallite are mostly disappeared. The percentages of the crystallites (X_c) of HC- and SC-PLA is calculated from the intensity ratios of the diffraction peaks of the HC and SC crystallites to the entire diffraction. The X_c value of HC decreases when the L/D ratio changes from 10/0 to 5/5, and then increases when the L/D ratio reaches to 0/10 (**Fig. 4b** blue). Conversely, X_c of SC increases (decreases) as that of HC decreases (increases) (**Fig. 4b** red).

PXRD measurements were further conducted upon elevating the temperature from 25 to 220 °C (**Fig. S3**). For the samples with the L/D ratios of 10/0, 1/9, 9/1, and 0/10, the diffraction peaks of the HC crystallite disappear at 200 °C due to the melting of the HC crystallites. For samples with the L/D ratios of 7/3, 5/5, and 3/7, small diffraction peaks from the HC crystallite remain at 200 °C, but they completely disappear at 220 °C. In contrast, diffraction peaks of the SC crystallites remain even at 220 °C. These results are consistent with the DSC results, where T_m of HC-PLA is around 180 °C while that of SC-PLA is around 230 °C.[47] **Figure 4c–f** plots the X_c values versus temperature for the HC and SC crystallites. X_c of the HC crystallites abruptly drops at 200 °C, and simultaneously, X_c of the SC crystallites increase at 200 °C. These results indicate that the melting of the HC domain subsequently induces the formation of the SC domains.

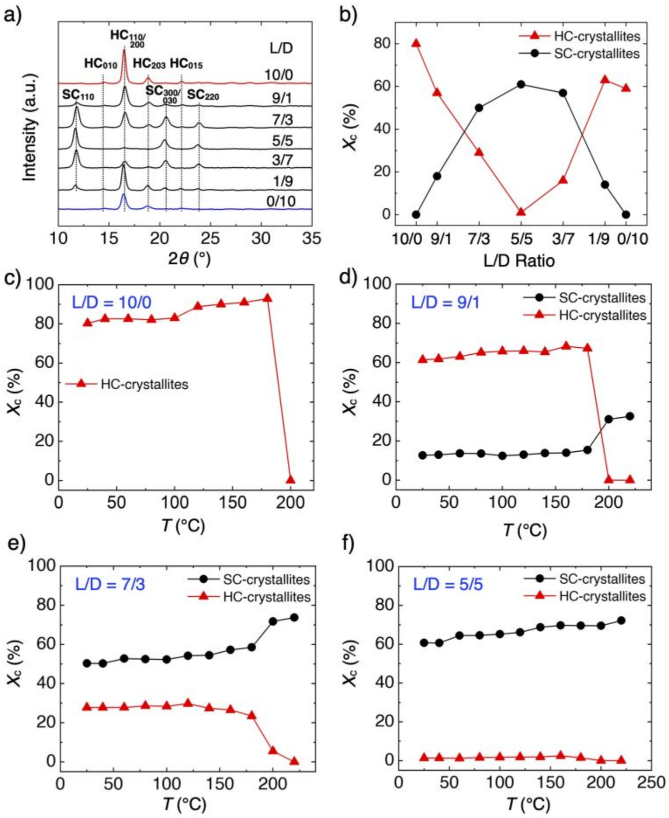

Fig. 4. (a) PXRD patterns of HC- and SC-PLA microsphere. (b) The relative degree of crystallinity (X_c) of the HC and SC crystallites. (c–f) Relative degree of X_c versus temperature in the range from 25 to 220 °C for HC and SC crystallites of PLA with the L/D ratio of 10/0 (c), 9/1 (d), 7/3 (e), and 5/5 (f).

The microspherical structure with smooth surface is advantageous for utilizing as a WGM optical resonator.[48–50] As schematically drawn in **Fig. 5a**, photoluminescence (PL) generated at the surface of the polymer microsphere is confined via total internal reflection at the medium/air interface and interfere by themselves to show up sharp and periodic resonant PL lines.[51–58] To investigate the optical resonator properties of the PLA microspheres, HC- and SC-PLA microspheres are doped with a fluorescent dye, zinc(II) tetraphenylporphyrin (ZnTPP), with T_m (~ 350 °C) higher than that of PLA. The ZnTPP-doped HC- or SC-PLA microspheres are dispersed on a quartz substrate by a spin coating method. PL spectra of a single HC- and SC-PLA microsphere are measured upon focused laser excitation with 405-nm continuous wave (cw) laser to a single microsphere.[59–63] At 30 °C, PL spectra from a HC-PLA microsphere involves periodic PL lines, attributed to WGMs (**Fig. 5b**). As shown in **Fig. S4**, these resonant peaks are assigned as transverse electric (TE) and transverse magnetic (TM) modes. The free spectral range (FSR) of four microspheres with different sizes are plotted in **Fig. S5**. FSR follows with an equation,

$$\mathrm{FSR} = (\lambda^2/n\pi)\bullet(1/d)$$

indicating that the PLA microspheres certainly act as an optical resonator.[64] The clear WGM peaks in the PL spectra is maintained upon thermal heating of the microspheres up to 160 °C (**Fig. S6a** in more detail). By further heating at 170 °C, these WGM PL peaks disappear due to the melting of HC-PLA that causes the deformation of the microspherical morphology.

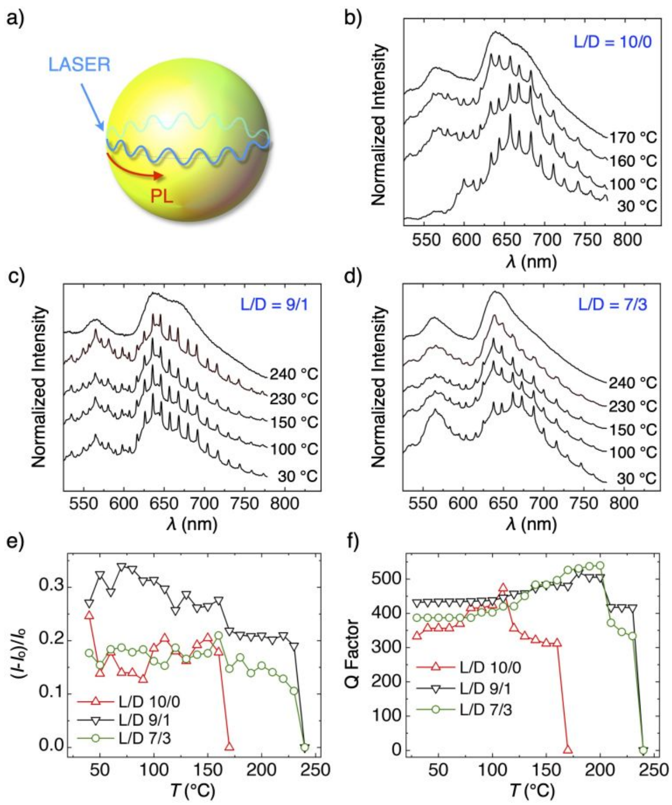

Fig. 5. (a) Schematic representation of the light confinement and WGM PL. (b–d) PL spectra of a single PLA microsphere after being annealed for 2 s upon photoexcitation at 405 nm with a cw laser. (e) Plots of the normalized PL intensity of the microspheres with L/D = 10/0, 9/1, and 7/3 versus annealing temperature. (f) Plots of Q factor of the microspheres with L/D = 10/0, 9/1, and 7/3 versus annealing temperature.

The optical resonator properties are observed for microspheres of SC-PLA with L/D of 9/1 and 7/3 (**Fig. 5c and d**, respectively). Intriguingly, the thermal stability of the microresonator preserves upon thermal heating up to 230 °C. The WGM PL peaks disappear by heating the microspheres at 240 °C (**Fig. S6b and c** in more detail). In **Fig. 5e**, temperature dependencies of the WGM peak intensity, normalized by the PL intensity of the background unconfined PL, are plotted. It is obvious that the thermal stability of the optical resonator is higher by ~70 °C for the microspheres of SC-PLA with L/D of 9/1 and 7/3 than that of the HC-PLA microspheres (L/D = 10/0). It is worth noting that the phase transition of PLA affects the shape of PL spectra, possibly caused by the change of the aggregation manner of ZnTPP in the PLA microspheres. We confirm that the ratio of the PL intensity at 603 and 643 nm (I_{603}/I_{643}) from a cast film of the PLA microspheres varies at the phase transition temperature (**Fig. S7**).

To gain insight into the resonant properties in more details, Q factor, defined as the wavelength of the resonant peaks divided by its full width at the half maximum (FWHM), are evaluated.[65] **Fig. 5f** plots Q factor of the PL peaks versus the heating temperature. Q factors gradually increases upon heating, possibly due to the improvement of the surface roughness. However, phase transition causes the loss of Q factors caused by the scattering of the confined light by the crystalline domains. For example, Q factor of the HC-PLA microsphere (L/D = 10/0) dropped from 500 to 360 at 110 °C, where phase transition occurs from glass to the crystalline state. Further drop of Q factor occurs at 170 °C, where melting of the HC-PLA takes place with the collapse of the microspherical morphology. In case of SC-PLA with L/D of 9/1 and 7/3, Q factors drop once at ~200 °C, where HC-PLA crystallites melt and SC-PLA crystallites form, and finally drop off at 240 °C, at which the SC-PLA completely melts.

For comparison, SC-PLA microspheres with L/D of 5/5, 3/7, and 1/9 display quite poor WGM PL (**Fig. S8**), because the surface morphology of the microspheres is rather rough with the RMS roughness greater than 6 (**Fig. 2**). The light confinement is sensitive to the surface roughness, where the rough surface causes a scatter of the confined light, leading to the loss of the optical resonator property.[65] Similarly, HC-PLA microspheres from PDLA (L/D = 0/10) does not show WGM PL due to the ill-defined spherical morphology (**Fig. S8**).

In conclusion, we successfully prepared thermally tolerant optical resonator from stereocomplex crystallites of PLA formed by blending of PLLA and PDLA through oil-in-water miniemulsion method. The SC-PLA microspheres exhibit the higher thermal stability in comparison with the HC-PLA microspheres, where the melting temperature of SC-PLA is more than 50 °C higher than that of HC-PLA. The relative degree of crystallinity of SC-PLA shows maximum when the content of PLLA and PDLA is 5/5, as evaluated by the PXRD studies. The temperature dependent PXRD results clearly show that PLAs maintain the stereocomplex structure even the temperature reaches to 220 °C. The temperature-dependent μ-PL spectroscopy shows that the SC-PLA resonators exhibit high thermal tolerance in comparison with the HC-PLA resonator, where the WGM resonance properties of SC-PLA preserve even at 230 °C. This work demonstrates the powerful strategy of the stereocomplex formation toward thermally tolerant bio-related materials for optical applications.

Conflicts of interest

There are no conflicts to declare.

Acknowledgements

This work was financially supported by CREST (JPMJCR20T4) and ACT-X (JPMJAX201J) from Japan Science and Technology Agency (JST), Grant-in-Aid for Scientific Research for Early-Career Scientists (JP22K14656) from Japan Society for the Promotion of Science (JSPS) and the New Energy and Industrial Technology Development Organization (NEDO), and Kato Memorial Bioscience Foundation.

References

1 A.P. Dove, Controlled ring-opening polymerisation of cyclic esters: Polymer blocks in self-assembled nanostructures. *Chem. Commun*., 2008, 48, 6446–6470.
2 Y. Baimark, W. Rungseesantivanon, and N. Prakymoramas, Preparation of stereocomplex-polylactide powder by precipitation method for potential use as nucleating agents in fully-biodegradable poly(L-lactide) composites. *Mater. Today Commun*., 2022, **33**, 1-8.
3 S. Inkinen, M. Stolt, and A. Södergård, Readily controllable step-growth polymerization method for poly(lactic acid) copolymers having a high glass transition temperature. *Biomacromolecules*, 2010, **11**, 1196–1201.
4 D. A. S. Marques, S. Jarmelo, C. M. S. G. Baptista, and M. H. Gil, Poly(lactic acid) synthesis in solution polymerization. *Macromol. Symp.*, 2010, **296**, 63–71.
5 S. Zhang, D. Yan, L. Zhao, and J. Lin, Composite fibrous membrane comprising PLA and PCL fibers for biomedical application. *Compos. Commun*., 2022, **34**, 101268.
6 T. A. M. Valente,D. M. Silva, P.S. Gomes, M. H. Fernandes, J. D. Santos, and V. Sencadas, Effect of sterilization methods on electrospun poly(lactic acid) (PLA) fiber alignment for biomedical applications. *ACS Appl. Mater. Interfaces*, 2016, **8**, 3241–3249.
7 M. Ekinci, C. C. Dos Santos, L. M. R. Alencar, H. Akbaba, R. Santos-Oliveira, D. and Ilem-Ozdemir, Atezolizumab-Conjugated Poly(lactic acid)/Poly(vinyl alcohol) Nanoparticles as Pharmaceutical Part Candidates for Radiopharmaceuticals. *ACS Omega*, 2022, **7**, 47956–47966.
8 E. Ibrahim, K. Taylor, S. Ahmed, A. Mahmud, K. Lozana, Centrifugally spun poly(D,L-lactic acid)-alginate composite microbeads for drug delivery and tissue engineering, *Int. J. Biol. Macromol*., 2023, **237**, 1-14.
9 S. Padee, S. Thumsorn, J. W. On, P. Surin, C. Apawet , T. Chaichalermwong, N. Kaabbuathong, T. O-Charoen, and N. Srisawat, Preparation of poly(lactic acid) and poly(trimethylene terephthalate) blend fibers for textile application. *Energy Procedia*, 2013, **34**, 534–541.
10 E. Bianchi, G. Guidotti, M. Soccio, V. Siracusa, M. Gazzano, E. Salatelli, and N. Lotti, Biobased and Compostable Multiblock Copolymer of Poly(l-lactic acid) Containing 2,5-Furandicarboxylic Acid for Sustainable Food Packaging: The Role of Parent Homopolymers in the Composting Kinetics and Mechanism. *Biomacromolecules*, 2023, **24**, 2356−2368
11 J. Jacob, V. Robert, R. B. Valapa, S. Kuriakose, S. Thomas, and S. Loganathan, Poly(lactic acid)/Polyethylenimine Functionalized Mesoporous Silica Biocomposite Films for Food Packaging. *ACS Appl. Polym. Mater*., 2022, **4**, 4632−4642.
12 G. Liu, X. Zhang, and D. Wang. Tailoring crystallization: Towards high-performance poly (lactic acid). *Adv. Mater.*, 2014, **26**, 6905–6911.
13 T. R. Cooper, and R. F. Storey, Poly(lactic acid) and chain-extended poly(lactic acid)-polyurethane functionalized with pendent carboxylic acid groups. *Macromolecules*, 2008, **41**, 655–662.
14 G. Mattana, D. Briand, A. Marette, A. V. Quintero, N. F. D. Rooij, Polylactic acid as a biodegradable material for all-solution-processed organic electronic devices, *Org. Electron.,* 2015, **17**, 77-86.
15 H. Zhao, Y. Bian, M. Xu, C. Han, Y. Li, Q. Dong, L. Dong, Enhancing the crystallization of poly(L-lactide) using a montmorillonitic substrate favoring nucleation. *CrystEngComm*, 2014, **16**, 3896–3905.
16 M. Aouay, A. Magnin, J. L. Putaux, and S. Boufi, Enhancing mechanical and thermal properties of plasticized poly-L-(lactic acid) by incorporating aminated-cellulose nanocrystals. *Ind. Crops Prod.*, 2023, **202**, 1–10.
17 X. Zhang, B. Yang, B. Fan, H. Sun, H. Zhang, Enhanced Nonisothermal Crystallization and Heat Resistance of Poly(l -lactic acid) by d -Sorbitol as a Homogeneous Nucleating Agent. *ACS Macro Lett.*, 2021, **10**, 154−160.
18 Y. Baimark, P. Srihanam, Y. Srisuwan, and T. Phromsopha, Enhancement in Crystallizability of Poly(L-Lactide) Using Stereocomplex-Polylactide Powder as a Nucleating Agent. *Polym.*, 2022, **14**, 1–14.
19 S. Kadea, T. Kittikorn, R. Chollakup, R. Hedthong, S. Chumprasert, N. Khanoonkon, S. Witayakran, and P. Chatakanonda, Influences of epoxidized natural rubber and fiber modification on injection molded-pulp/poly(lactic acid) biocomposites: Analysis of mechanical-thermal and weathering stability. *Ind. Crops Prod.*, 2023, **201**, 1–10.
20 J. Feng, Y. Sun, P. Song, W. Lei, Q. Wu, L. Liu, Y. Yu, and H. Wang, Fire-Resistant, Strong, and Green Polymer Nanocomposites Based on Poly(lactic acid) and Core-Shell Nanofibrous Flame Retardants. *ACS Sustainable Chem. Eng.*, 2017, **5**, 7894−7904.
21 Y. Li, L. Zhao, C. Han, and L. Xiao, Thermal and mechanical properties of stereocomplex polylactide enhanced by nanosilica. *Colloid Polym. Sci.*, 2021, **299**, 1161–1172.
22 M. Tesfaye, R. Patwa, P. Dhar, and V. Katiyar, Nanosilk-grafted poly(lactic acid) films: Influence of cross-linking on rheology and thermal stability. *ACS Omega*. 2017, **2**, 7071−7084.
23 H. Tsuji, S. Sato, N. Masaki, Y. Arakawa, Y. Yoshizaki, A. Kuzuya, and Y. Ohya, Thermal properties and degradation of enantiomeric copolyesteramides poly(lactic acid-co-alanine)s. *Polym. Degrad. Stab.*, 2020, **171**, 1–9.
24 F. Tang, and Y. G. Jeong, Improvement in thermal stability, elastic modulus, and impact strength of Poly(lactic acid) blends with modified polyketone. *Polym.*, 2022, **257**, 1–9.
25 B. Ma, H. Zhang, K. Wang, H. Xu, Y. He, and X. Wang, Influence of scPLA microsphere on the crystallization behavior of PLLA/PDLA composites. *Compos. Commun.*, 2020, **21**, 1–6.
26 M. Guo, W. Wu, W. Wu, and Q. Gao, Competitive Mechanism of Stereocomplexes and Homocrystals in High-Performance Symmetric and Asymmetric Poly(lactic acid) Enantiomers: Qualitative Methods. *ACS Omega*, 2022, **7**, 41412–41425.

27 Z. Gu, Y. Xu, Q. Lu, C. Han, R. Liu, Z. Zhou, T. Hao, and Y. Nie, Stereocomplex formation in mixed polymers filled with two-dimensional nanofillers. *Phys.Chem.Chem.Phys.*, 2019, **21**, 6443–6452.
28 W. Li W, Q. Ren, H. Zhu, M. Wu, Z. Weng, L. Wang, and W. Zheng, Enhanced heat resistance and compression strength of microcellular poly (lactic acid) foam by promoted stereocomplex crystallization with added D-Mannitol. *J. CO_2 Util.*, 2022, **63**, 1–11.
29 J. Hirata, N. Kurokawa, M. Okano, A. Hotta, and S. Watanabe, Evaluation of Crystallinity and Hydrogen Bond Formation in Stereocomplex Poly(lactic acid) Films by Terahertz Time-Domain Spectroscopy. *Macromolecules*, 2020, **53**, 7171–7177.
30 M. Guo, W. Wu, W. Wu, R. Wang, L. Huang, and Q. Gao, Recent advances in enhancing stereocomplexation between poly(lactide) enantiomeric chains. *Phys. Chem. Chem. Phys.*, 2023,**25**, 17737–17758.
31 M. Fujita M, T. Sawayanagi, H. Abe, T. Tanaka, T. Iwata, K. Ito, T. Fujisawa, and M. Maeda, Stereocomplex formation through reorganization of poly(L-lactic acid) and poly(D-lactic acid) crystals. *Macromolecules*, 2008, **41**, 2852–2858.
32 B. Yu B, L. Meng, S. Fu, Z. Zhao, Y. Liu, K. Wang, and Q. Fu, Morphology and internal structure control over PLA microspheres by compounding PLLA and PDLA and effects on drug release behavior. *Colloids Surf. B*, 2018, **172**, 105–12.
33 L. Feng, X. Bian, G. Li, and X. Chen, Compatibility and Thermal and Structural Properties of Poly(l -lactide)/Poly(l - Co- d -lactide) Blends. *Macromolecules*, 2022, **55**, 1709–1718.
34 S. Nouri, C. Dubois, and P. G. Lafleur, Homocrystal and stereocomplex formation behavior of polylactides with different branched structures. *Polym.*, 2015, **67**, 227–239.
35 J. Sun, J. Shao, S. Huang, B. Zhang, G. Li, X. Wang, and X. Chen, Thermostimulated crystallization of polylactide stereocomplex. *Mater. Lett.*, 2012, **89**, 169–171.
36 Jiang X, Yang L. Optothermal dynamics in whispering-gallery microresonators. *Light: Sci. Appl.,* 2020, **9**, 24.
37 A. R. Anwar, M. Mur, and M. Humar, Microcavity- and Microlaser-Based Optical Barcoding: A Review of Encoding Techniques and Applications, *ACS Photon.,* 2023, **10**, 1202−1224.
38 T. N. Pham, S. Guerrault, and C. Ayela, Polymer Microtip Based Fabry−Perot Interferometer for Water Content Determination in the Gas and Liquid Phase, *ACS Appl. Mater. Interfaces*, 2023, **15**, 46368−46378.
39 M. Loyez, M. Adolphson, J. Liao, and L. Yang, From Whispering Gallery Mode Resonators to Biochemical Sensors, *ACS Sens.*, 2023, **8**, 2440−2470.
40 Y. C. Tao, X. D. Wang, and L. S. Liao, Active whispering-gallery-mode optical microcavity based on self-assembled organic microspheres, *J. Mater. Chem. C*, 2019, **7**, 3443–3446.
41 G. C. Righini GC, and S. Soria, Biosensing by WGM microspherical resonators. *Sensors*, 2016, **16**, 905.
42 N. Toropov, G. Cabello, M. P. Serrano, R. R. Gutha, M. Rafti, and F. Vollmer, Review of biosensing with whispering-gallery mode lasers, *Light: Sci. Appl.,* 2021, **10**, 42.
43 S. H. Im, S. J. Park, Y. Jung, J. J. Chung, and S. H. Kim, Strategy for Stereocomplexation of Polylactide Using O/W Emulsion Blending and Applications as Composite Fillers, Drug Carriers, and Self-Nucleating Agents. *ACS Sustain. Chem. Eng.*, 2020, **8**, 8752–8761.
44 L. Feng, X. Bian, G. Li, and X. Chen. Thermal Properties and Structural Evolution of Poly(l -lactide)/Poly(d -lactide) Blends. *Macromolecules*. 2021, **54**, 10163–10176.
45 Y. Kong, and J. N. Hay, The enthalpy of fusion and degree of crystallinity of polymers as measured by DSC. *Eur. Polym J.*, 2003, **39**, 1721–1727.
46 B. Ma, H. Zhang, K. Wang, H. Xu, Y. He, and X. Wang, Influence of scPLA microsphere on the crystallization behavior of PLLA/PDLA composites. *Compos. Commun.*, 2020, **21**, 1-6.
47 K. Tashiro, N. Kouno, H. Wang, and H. Tsuji, Crystal Structure of Poly(lactic acid) Stereocomplex: Random Packing Model of PDLA and PLLA Chains As Studied by X-ray Diffraction Analysis. *Macromolecule*s, 2017, **50**, 8048–8065.
48 Y. Yamamoto, Spherical resonators from π-conjugated polymers, *Polym. J.* ,2016, **48**, 1045–1050.
49 Y. Yamamoto, H. Yamagishi, J. S. Huang, and A. Lorke, Molecular and Supramolecular Designs of Organic/Polymeric Micro-photoemitters for Advanced Optical and Laser Applications, *Acc. Chem. Res.*, 2023, **56**, 1469−1481.
50 Y. Yamamoto, S. Kushida, D. Okada, O. Oki, H. Yamagishi, and Hendra. Self-Assembled π-Conjugated Organic/Polymeric Microresonators and Microlasers. *Bull. Chem. Soc. Jpn.*, 2023, **96**, 702-710.
51 K. Tabata, D. Braam, S. Kushida, L. Tong, J. Kuwabara, T. Kanbara, and Y. Yamamoto, Self-assembled conjugated polymer spheres as fluorescent microresonators. *Sci. Rep.*, 2014, **4**, 1-4.
52 D. Okada, T. Nakamura, D. Braam, T. D. Dao, S. Ishii, T. Nagao, A. Lorke, T. Nabeshima, and Y. Yamamoto, Color-Tunable Resonant Photoluminescence and Cavity-Mediated Multistep Energy Transfer Cascade. *ACS Nano*, 2016, **10**, 7058−7063.
53 S. Kushida, D. Braam, T. D Dao, H. Saito, K. Shibasaki, S. Ishii S, T. Nagao, A. Saeki, J. Kuwabara, T. Kanbara, M. Kijima, A. Lorke, and Y. Yamamoto, Conjugated Polymer Blend Microspheres for Efficient, Long-Range Light Energy Transfer. *ACS Nano*, 2016, **10**, 5543–5549.
54 M. Gao, C. Wei, X. Lin, Y. Liu, F. Hu, Y. S. Zhao, Controlled assembly of organic whispering gallery-mode microlasers as highly sensitive chemical vapor sensors, *Chem. Commun*., 2017, 53, 3102.
55 R. Vattikunta, D. Venkatakrishnarao, C. Sahoo, S. R. G. Naraharisetty, D. N. Rao, Klaus Mullen, and R. Chandrasekar, Photonic Microresonators from Charge Transfer in Polymer Particles: Toward Enhanced and Tunable Two-Photon Emission, *ACS Appl. Mater. Interfaces*, 2018, **10**, 16723−16730.
56 D. Venkatakrishnarao, C. Sahoo, R. Vattikunta, M. Annadhasan, S. R. G. Naraharisetty, and R. Chandrasekar, 2D Arrangement of Polymer Microsphere Photonic Cavities Doped with Novel N-Rich Carbon Quantum Dots Display Enhanced One- and Two-Photon Luminescence Driven by Optical Resonances, *Adv. Opt. Mater*., 2017, **5**, 1700695.
57 M. Annadhasan, A. V. Kumar, D. Venkatakrishnarao, E. A. Mamonov and R. Chandrasekar, Mechanophotonics: precise selection, assembly and disassembly of polymer optical microcavities via mechanical manipulation for spectral engineering, *Nanoscale Adv*., 2020, **2**, 5584.
58 Radhika Vattikunta, Mari Annadhasan, Ravi Jada, Muvva Durga Prasad, Nikolai Mitetelo, Karina Zhdanova, Evgeniy Mamonov, Klaus Müllen, Tatiana Murzina, and Rajadurai Chandrasekar, Multifunctional Chiral π-Conjugated Polymer Microspheres: Production and Confinement of NLO signal, Detection of Circularly Polarized Light, and Display of Laser-Triggered NLO Emission Shifts, *Adv. Opt. Mater*., 2020, **8**, 2000431.
59 S. Kushida, D. Braam, C. Pan, T. D. Dao, K. Tabata, K. Sugiyasu, M. Takeuci, S. Ishii, T. Nagao, A. Lorke, and Y. Yamamoto, Whispering Gallery Resonance from Self-Assembled Microspheres of Highly Fluorescent Isolated Conjugated Polymers. *Macromolecules*, 2015, **48**, 3928–3933.
60 W. Y. Heah, H. Yamagishi, K. Fujita, M. Sumitani, Y. Mikami, H. Yoshioka, Y. oki, and Y. Yamamoto, Silk fibroin microspheres as optical resonators for wide-range humidity sensing and

biodegradable lasers. *Mater. Chem. Front.*, 2021, **5**, 5653–5657.
61 N. Tanji, H. Yamagishi, K. Fujita, and Y. Yamamoto, Nanoporous Fluorescent Microresonators for Non-wired Sensing of Volatile Organic Compounds down to the ppb Level. *ACS Appl. Polym. Mater.*, 2022, **4**, 1065–1070.
62 Hendra, A. Takeuchi, H. Yamagishi, O. Oki, M. Morimoto, M. Irie, and Y. Yamamoto, Photochemically Switchable Interconnected Microcavities for All-Organic Optical Logic Gate. *Adv. Funct. Mater.*, 2021, **31**, 1-7.
63 Hendra, H. Yamagishi, W. Y. Heah, A. D. Malay, K. Numata, and Y. Yamamoto, Micrometer-Scale Optical Web Made of Spider Dragline Fibers with Optical Gate Operations. *Adv. Opt. Mater.*, 2022, **11**, 2202563.
64 L. Cai, J. Pan, Y. Zhao, J. Wang, and S. Xiao, Whispering gallery mode optical microresonators: Structures and sensing applications, *Phys. Status Solidi A*, 2020, **217**, 1900825.
65 O. Oki, S. Kushida, A. Mikosch, K. Hatanaka, Y. Takeda, S. Minakata, J. Kuwabara, T. Kanbara, T. D. Dao, S. Ishii, T. NAGAO, A. Kuehne, F. Deschler, R. Friend, and Y. Yamamoto, FRET-mediated near infrared whispering gallery modes: Studies on the relevance of intracavity energy transfer with Q-factors. *Mater. Chem. Front.*, 2018, **2**, 270–274.